Electronic Supplementary Information

Imine bond orientation manipulates AIEgens derived Schiff bases isomers through intramolecular hydrogen bond effect for different fluorescent properties and applications

Da Li[a], Xiaozhong Liang[a], Fang Zhang[b], Jie Li[a], Zheng Zhang[a], Sijing Wang[a], Zhijun Li[a], Yifan Xing[a], Kunpeng Guo[a]*

a Ministry of Education Key Laboratory of Interface Science and Engineering in Advanced Materials, Research Center of Advanced Materials Science and Technology, Taiyuan University of Technology, Taiyuan, 030024, China

b Department of Energy Chemistry and Materials Engineering, Shanxi Institute of Energy, Jinzhong, 030600, China.

Contents

Experimental section

1.1 Materials and instruments

4'-(1,2,2-triphenylvinyl) biphenyl-4-amine (**1NA**), 4-(2-thienyl) aniline (**3NA**), 4'-(1,2,2-triphenylethenyl) biphenyl-4-formaldehyde (**1CA**), and 4'-(diphenylamino)-[1,1'-biphenyl]-4-carbaldehyde (**2CA**) were purchased from Zhengzhou Alpha Chemical Co. LTD. N, N-diphenylbenzidine (**2NA**) and 4-(2-thienyl) benzaldeyde (**3CA**) were supplied by Shenzhen Atomax Chemical Co. LTD. All chemicals and reagents involved in this work were used directly as obtained commercially unless otherwise stated.

NMR spectra measurements were carried out at a Bruker NMR 600 MHz for ^{1}H NMR and 150 MHz for ^{13}C NMR, using DMSO-*d*6, $CDCl_3$ and acetone-*d*6 as solvents. Chemical shifts were reported in parts per million (ppm) relative to internal TMS (0 ppm). Splitting patterns were described as singlet (s), doublet (d), triplet (t), quartet (q), or multiplet (m). Mass spectra measured on Microflex MALDI-TOF MS. Single-crystal X-ray diffraction data were collected on an Agilent SuperNova (Dual, Cu at zero, Eos) diffractometer. The crystal was kept at 173.00 (10) K during data collection. Using Olex2, the structure was solved with the ShelXS structure solution program using Direct Methods and refined with the ShelXL refinement package using least-squares technique. UV-Vis spectra were recorded in a HITIACH U-3900 spectrometer. Photoluminescent (PL) spectra were recorded in a HITACHI F-4700 spectrofluorometer. Theoretical calculations using density functional theory (DFT) were performed using the Gaussian09 package at the B3LYP/6-31G(d) level.

1.2 Synthesis

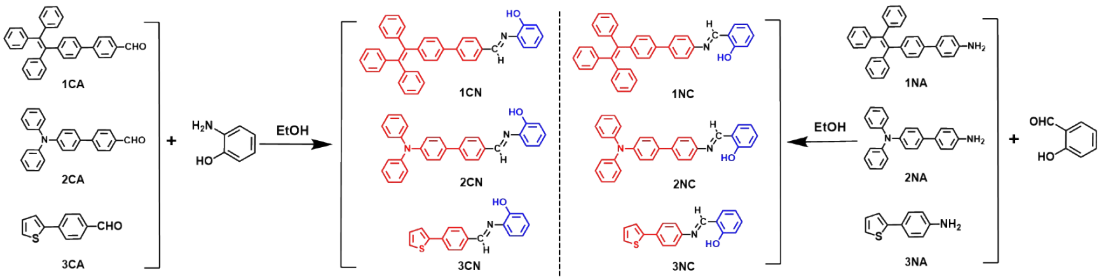

Scheme S1 Synthetic routes of **1–3NC** and **1–3CN**.

Synthesis of 1NC ((E)-2-(((4'-(1,2,2-triphenylvinyl)-[1,1'-biphenyl]-4-yl) imino) methyl) phenol)

A solution of **1NA** (120 mg, 0.28 mmol) and salicylaldehyde (70 mg, 0.57 mmol) in anhydrous ethanol (15 mL) was stirred under reflux for 6 h. After filtration, **1NC** was afforded as light green solid (82 mg, yield 68.3%) by washing the precipitate several times with ethanol. ^{1}H NMR (600 MHz, DMSO-*d*6) δ (ppm): 13.11 (s, 1H), 9.03 (s, 1H), 7.74 (d, *J* = 8.4 Hz, 2H), 7.67 (d, *J* = 7.2 Hz, 1H), 7.51 (dd, *J* = 28.2, 8.4 Hz, 4H), 7.43 (t, *J* = 7.8 Hz, 1H), 7.15 (m, 10H), 7.04 (m, 5H), 6.98 (m, 4H). ^{13}C NMR (150 MHz, $CDCl_3$) δ (ppm): 162.17, 161.17, 147.35, 143.72, 143.70, 143.68, 143.03, 141.25, 140.42, 139.37, 137.91, 133.17, 132.27, 131.89, 131.42, 131.36, 127.80, 127.73, 127.66, 126.55, 126.53, 126.47, 126.03, 121.57, 119.27, 119.10, 117.28. MALDI-TOF: m/z [M]+ cacld. $C_{39}H_{29}NO$, 527.2210; found: 527.2209.

Synthesis of 1CN ((E)-2-(((4'-(1,2,2-triphenylvinyl)-[1,1'-biphenyl]-4-yl) methylene) amino) phenol)

A solution of **1CA** (120 mg, 0.27 mmol) and *o*-aminophenol (60 mg, 0.55 mmol) in anhydrous ethanol (15 mL) was stirred under reflux for 6 h. After filtration, **1CN** was afforded as light green solid (85 mg, yield 71%) by washing the precipitate several times with ethanol. ^{1}H NMR (600 MHz, DMSO-*d*6) δ (ppm): 8.99 (s, 1H), 8.71 (s, 1H), 8.05 (m, 2H), 7.76 (m, 2H), 7.57 (m, 2H), 7.20 (dd, *J* = 7.8, 1.8 Hz, 1H), 7.14 (m, 9H), 7.07 (m, 3H), 7.03 (m, 2H), 7.01 (m, 2H), 6.97 (m, 2H), 6.88 (dd, *J* = 8.4, 1.2 Hz, 1H), 6.82 (td, *J* = 7.2, 1.2 Hz, 1H). ^{13}C NMR (150 MHz, $CDCl_3$) δ (ppm): 156.58, 152.37, 143.84, 143.69, 143.65, 143.64, 143.61, 141.47, 140.31, 137.69, 135.56, 134.64, 131.98, 131.42, 131.36, 131.35, 129.24, 128.91, 127.83, 127.76, 127.68, 127.22, 126.62, 126.58, 126.53, 126.29, 120.13, 115.81, 115.00. MALDI-TOF: m/z [M]+ cacld. $C_{39}H_{29}NO$, 527.2210; found: 527.2207.

Synthesis of 2NC ((E)-2-(((4'-(diphenylamino)-[1,1'-biphenyl]-4-yl) imino) methyl) phenol)

The synthetic route of **2NC** was the same as that for **1NC**, except that **1NA** was replaced with **2NA**. After filtration, **2NC** was afforded as light yellow solid (103 mg,

yield 86%) by washing the precipitate several times with ethanol. ^{1}H NMR (600 MHz, DMSO-*d*6) δ (ppm): 13.17 (s, 1H), 9.04 (s, 1H), 7.75 (dt, *J* = 8.4 Hz, 2H), 7.67 (dd, *J* = 8.0, 5.8 Hz, 3H), 7.51 (dt, *J* = 8.4 Hz, 2H), 7.43 (ddd, *J* = 8.4, 7.2, 1.8 Hz, 1H), 7.34 (dd, *J* = 8.4, 7.2 Hz, 4H), 7.07 (m, 9H), 6.99 (m, 2H). ^{13}C NMR (150 MHz, $CDCl_3$) δ (ppm): 162.01, 161.17, 147.59, 147.40, 147.00, 139.40, 134.03, 133.12, 132.24, 129.32, 127.59, 127.51, 124.52, 123.78, 123.06, 121.64, 119.30, 119.09, 117.27. MALDI-TOF: m/z [M]+ cacld. $C_{31}H_{24}N_2O$, 440.1900; found: 440.1898.

Synthesis of 2CN ((E)-2-(((4'-(diphenylamino)-[1,1'-biphenyl]-4-yl) methylene) amino) phenol)

The synthetic route of **2CN** was the same as that for **1CN**, except that **1CA** was replaced with **2CA**. After filtration, **2CN** was afforded as yellow solid (98 mg; 82%) by washing the precipitate several times with ethanol. ^{1}H NMR (600 MHz, $CDCl_3$) δ (ppm): 8.73 (s, 1H), 7.97 (d, *J* = 1.2, 2H), 7.70 (d, *J* = 8.4, 2H), 7.54 (d, *J* = 7.2, 2H), 7.33 (dd, *J* = 7.8, 1.2 Hz, 1H), 7.29 (td, *J* = 7.3, 2.1 Hz, 5H), 7.20 (td, *J* = 4.8, 1H), 7.15 (m, 6H), 7.06 (td, *J* = 7.8, 1.2 Hz, 2H), 7.03 (dd, *J* = 8.4, 1.2 Hz, 1H), 6.92 (td, *J* = 7.8, 1.4 Hz, 1H). ^{13}C NMR (150 MHz, $CDCl_3$) δ (ppm): 160.01, 147.84, 147.50, 134.65, 129.35, 129.32, 129.16, 127.82, 126.79, 125.89, 124.65, 123.53, 123.21, 120.92. MALDI-TOF: m/z [M]+ cacld. $C_{31}H_{24}N_2O$, 440.1900; found: 440.1897.

Synthesis of 3NC ((E)-2-(((4-(thiophen-2-yl) phenyl) imino) methyl) phenol)

The synthetic route of **3NC** was the same as that for **1NC**, except that **1NA** was replaced with **3NA**. After filtration, **3NC** was afforded as yellow solid (95 mg; 79%) by washing the precipitate several times with ethanol. ^{1}H NMR (600 MHz, DMSO-*d*6) δ (ppm): 13.08 (s, 1H), 9.03 (s, 1H), 7.76 (dt, *J* = 8.4 Hz, 2H), 7.68 (dd, *J* = 7.8, 2.4 Hz, 1H), 7.58 (m, 2H), 7.49 (dt, *J* = 6.6 Hz, 2H), 7.43 (t, *J* = 7.8 Hz, 1H), 7.16 (dd, *J* = 5.4 Hz, 3.6 Hz, 1H), 6.99 (m, 2H). ^{13}C NMR (150 MHz, $CDCl_3$) δ (ppm): 162.17, 161.16, 147.47, 143.62, 133.23, 132.30, 128.18, 126.86, 125.08, 123.26, 121.76,119.23, 119.14, 117.29. MALDI-TOF: m/z [M]+ cacld. $C_{17}H_{13}NOS$, 279.0721; found: 279.0719.

Synthesis of 3CN ((E)-2-((4-(thiophen-2-yl) benzylidene) amino) phenol)

The synthetic route of **3CN** was the same as that for **1CN**, except that **1CA** was

replaced with **3CA**. After filtration, **3CN** was afforded as yellow solid (102 mg; 85%) by washing the precipitate several times with ethanol. ^{1}H NMR (600 MHz, acetone-*d*6) δ (ppm): (s, 1H), 8.11 (m, 2H), 8.02 (s, 1H), 7.82 (m, 2H), 7.61 (dd, *J* = 3.6, 1.2 Hz, 1H), 7.55 (dd, *J* = 3.6, 1.2 Hz, 1H), 7.42 (dd, *J* = 6.0, 1.8 Hz, 1H), 7.17 (m, 2H), 6.94 (dd, *J* = 8.0, 1.3 Hz, 1H), 6.89 (td, *J* = 7.2Hz, 1H). ^{13}C NMR (150 MHz, $CDCl_3$) δ (ppm): 156.25, 152.37, 143.37, 137.45, 135.50, 134.79, 129.42, 128.96, 128.36, 126.06, 124.21, 120.14, 115.80, 115.01. MALDI-TOF: m/z [M]+ cacld. $C_{17}H_{13}NOS$, 279.0721; found: 279.0720.

Synthesis of RC ((E)-1-(2-methoxyphenyl)-N-(4'-(1,2,2-triphenylvinyl)-[1,1'-biphenyl]-4-yl) methanimine)

The synthetic route of **RC** was the same as that for **1NC**, except that salicylaldehyde was replaced with 2-methoxybenzaldehyde. After filtration, **RC** was afforded as yellow solid (127 mg; 83.8%) by washing the precipitate several times with ethanol. ^{1}H NMR (600 MHz, DMSO-*d6*) δ (ppm) 8.66 (s, 1H), 7.71 (m, 3H), 7.49 (m, 2H), 7.44 (m, 5H), 7.37 (m, 17H), 7.05 (m, 2H), 3.87 (s, 3H). ^{13}C NMR (150 MHz, DMSO-*d6*) δ (ppm) 159.83, 159.60, 153.70, 153.16, 149.56, 142.47, 141.59, 139.60, 139.28, 138.89, 132.47, 131.36, 130.56, 130.54, 130.51, 128.96, 128.81, 128.23, 128.20, 128.17, 127.32, 127.28, 127.11, 126.37, 122.61, 122.23, 113.62, 55.78. MALDI-TOF: m/z [M]+ cacld. $C_{40}H_{31}NO$, 541.2410; found: 542.2410.

1.3 UV–vis and fluorescence spectroscopic analytical procedure

The stock solutions (2.5 mM) were obtained by dissolving the requisite amounts of **1–3NC** and **1–3CN** in acetone solvent, respectively. The standard stock solutions (10 mM) were prepared by dissolving the appropriate amount metal salts of Al^{3+}, Zn^{2+}, Fe^{3+}, Cu^{2+}, Ag^{+}, Hg^{2+}, Pb^{2+}, Cr^{3+}, Cd^{2+}, Ca^{2+}, Mg^{2+}, Na^{+}, K^{+}, Ni^{2+}, Mn^{2+}, Fe^{2+} and Co^{2+} in deionized water, respectively. UV–vis and fluorescence measurements were performed in a acetone/H_2O (v:v, 1:99) solution containing the tested compounds (**1–3NC** or **1–3CN,** 25 μM). Fluorescence and UV-vis spectra were measured after addition of the ions at room temperature to equilibrium. Fluorescence measurements were carried out with excitation of 365 nm.

1.4 Recovery experiments in real water samples

The real water samples including tap water and drinking water collected from Taiyuan University of Technology which need no further purification and river water collected from Fenhe River which should be filtered out of the suspended solids with filter paper. The recovery experiments were carried out by spiking the known concentrations of Al^{3+} (Zn^{2+}) into different water samples and then analyzing with the same detection method in triple replicates. The detected Al^{3+} (or Zn^{2+}) concentrations were calculated by the fluorescent response compared to that in corresponding deionized samples. Then, the recovery percentages were calculated to evaluate the degree of deviation of the detected value compared to the amount of spiked Al^{3+} (or Zn^{2+}).

1.5 Preparation of test papers

The test papers were obtained by soaking the filter paper in the acetone solution of the sensor (5 mM) and then removing for drying in the air. After metal ions were dripped on the test papers coated with **1–3NC** and **1–3CN** and dried in the air, different response patterns were observed under 365 nm UV lamp and quantized by the fluorescence spectra, respectively.

2. Figures

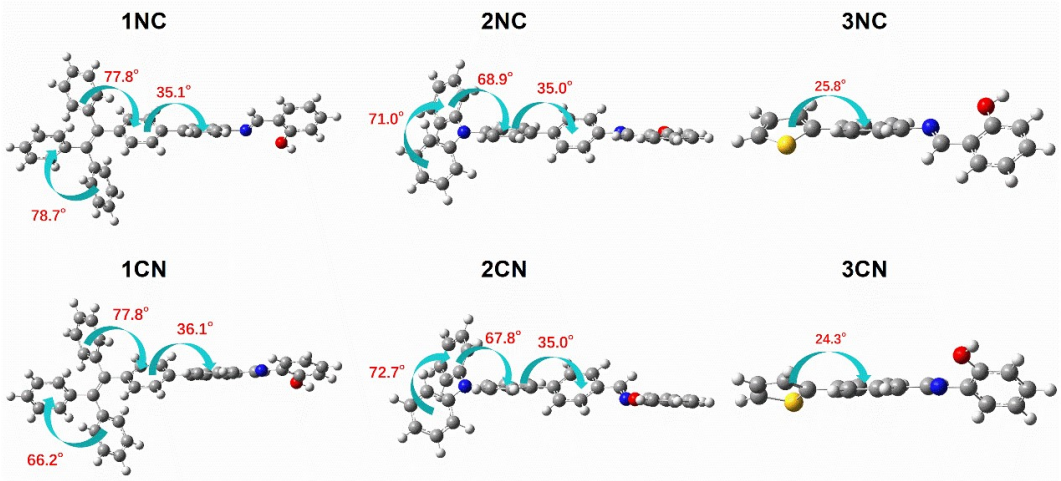

Fig. S1 Molecular structures and geometrically optimized 3D molecular models of **1–3NC** and **1–3CN** by DFT B3LYP/6-31G(d) calculation.

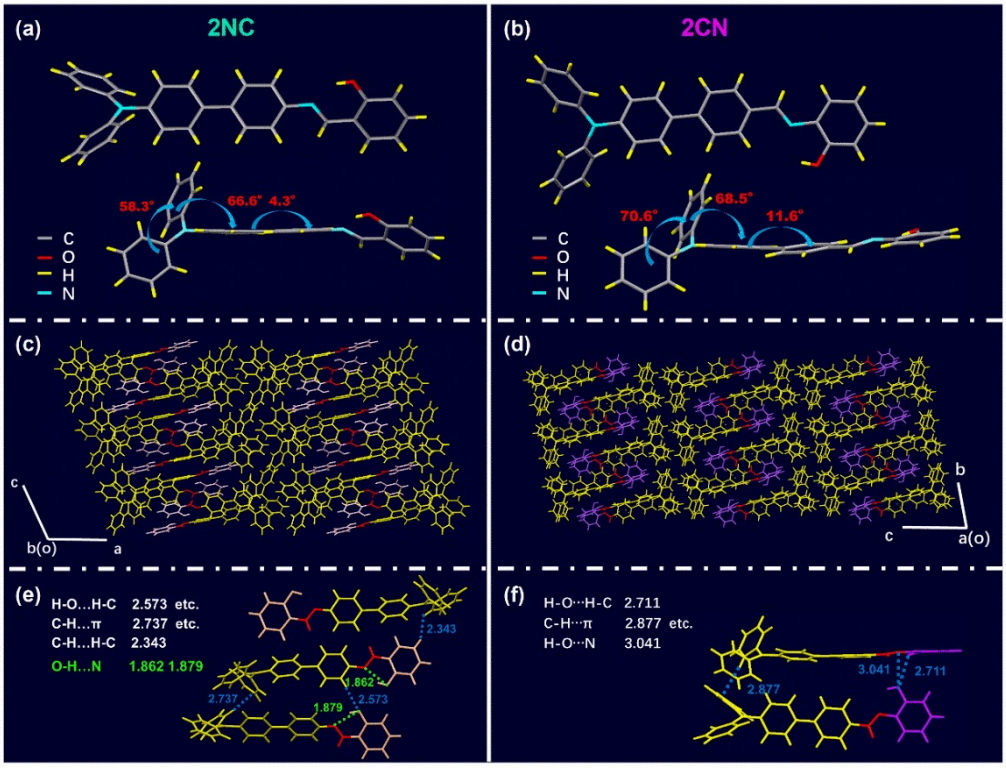

Fig. S2 Crystal structures of (a) **2NC** and (b) **2CN**. Molecular packing of (c) **2NC** and (d) **2CN** crystals. Multiple intermolecular and intramolecular interactions in crystals of (e) **2NC** and (f) **2CN** with indicated distances (Å).

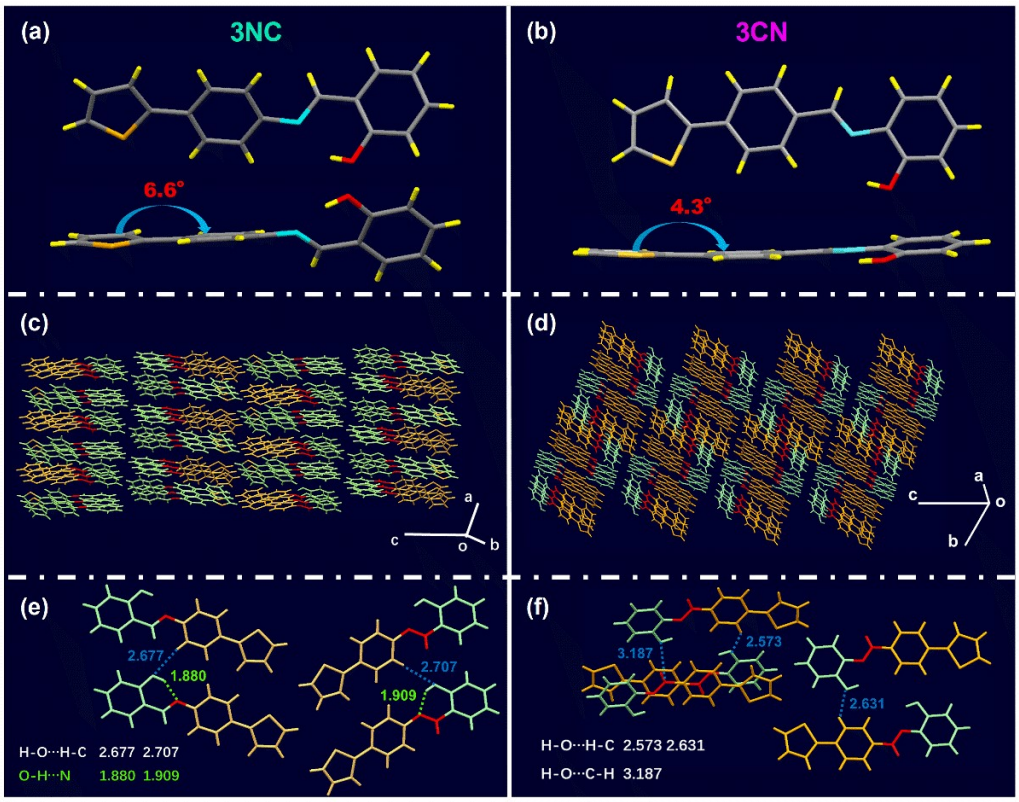

Fig. S3 Crystal structures of (a) **3NC** and (b) **3CN**. Molecular packing of (c) **3NC** and (d) **3CN** crystals. Multiple intermolecular and intramolecular interactions in crystals of (e) **3NC** and (f) **3CN** with indicated distances (Å).

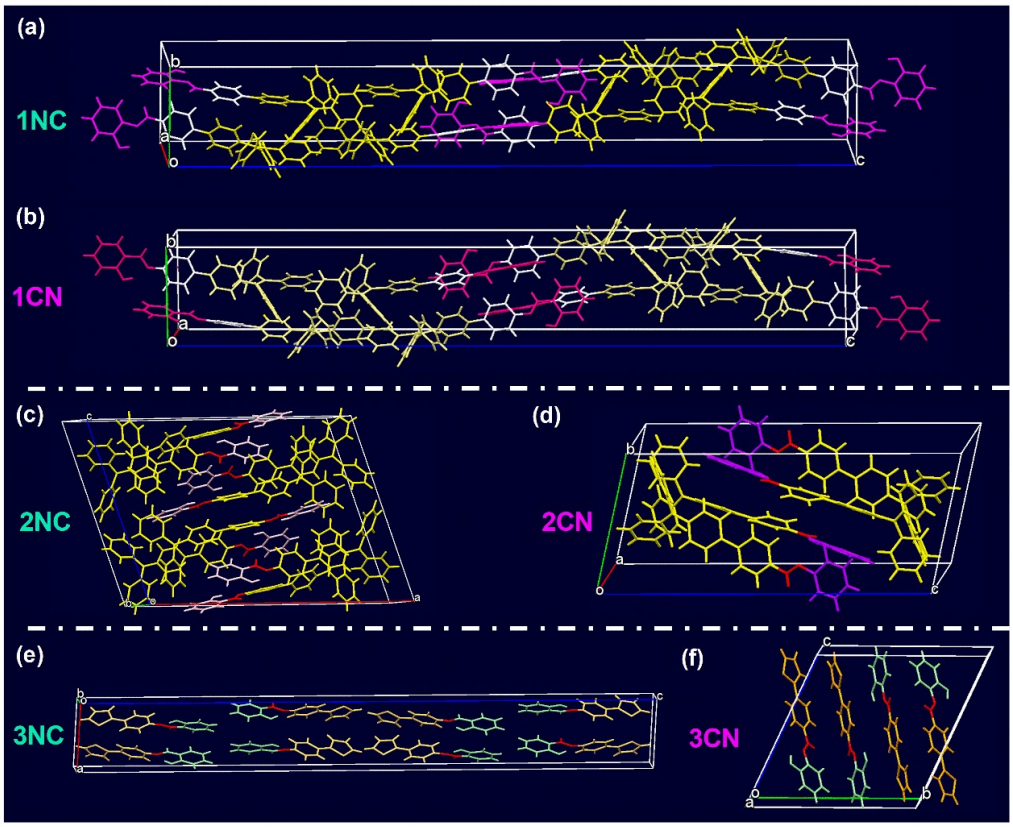

Fig. S4 Single cell units of (a) **1NC**, (b) **1CN**, (c) **2NC**, (d) **2CN**, (e) **3NC** and (f) **3CN**.

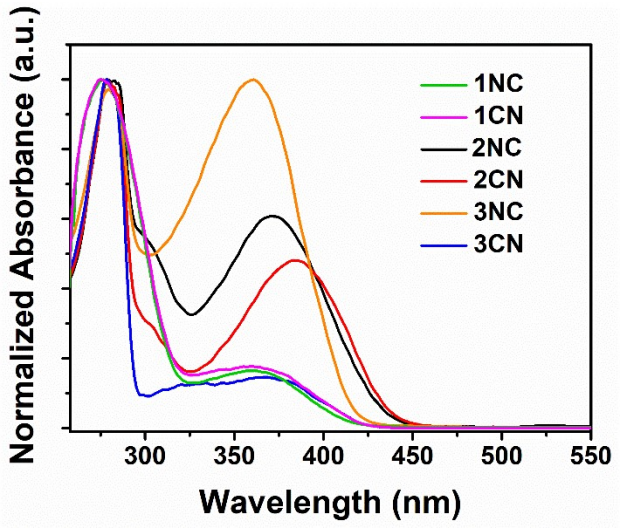

Fig. S5 Normalized absorption spectra of **1–3NC** and **1–3CN** in acetone solution (25 μM).

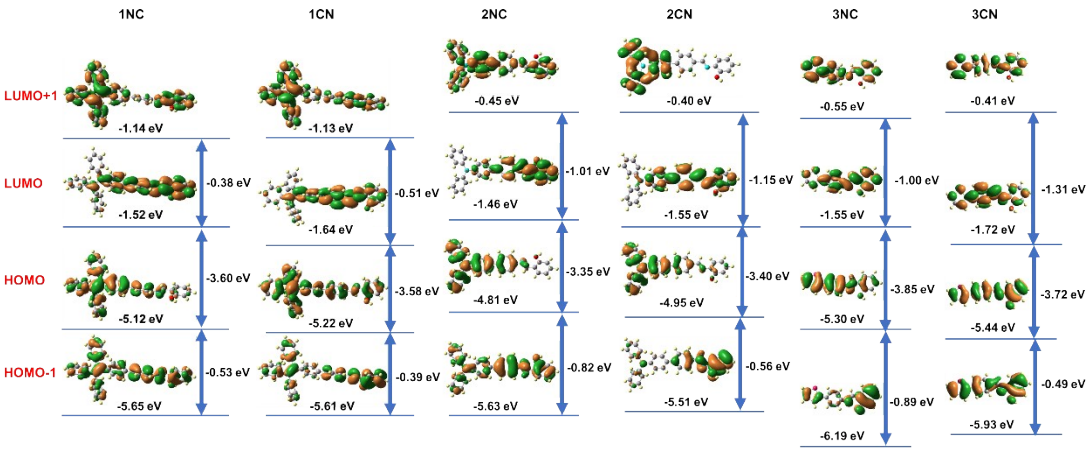

Fig. S6 Frontier molecular orbital diagram of **1–3NC** and **1–3CN** by DFT calculation.

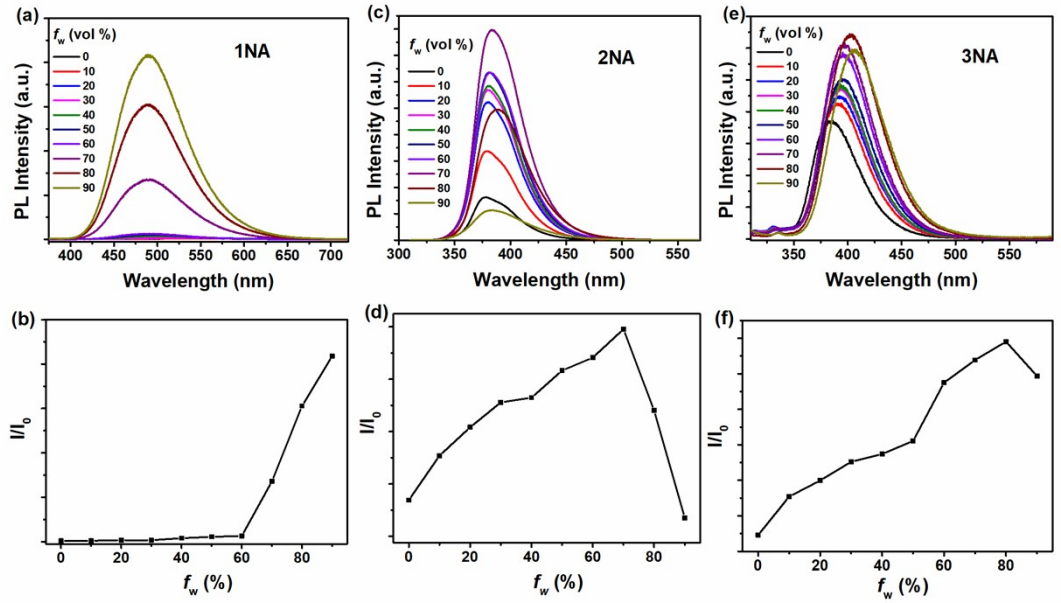

Fig. S7 PL spectra of (a) **1NA**, (c) **2NA**, (e) **3NA** in the mixture of acetone/H_2O (25 μM, f_w from 0 to 90%) and the corresponding variations in PL intensity (I/I_0) of (b) **1NA**, (d) **2NA**, (f) **3NA** with f_w.

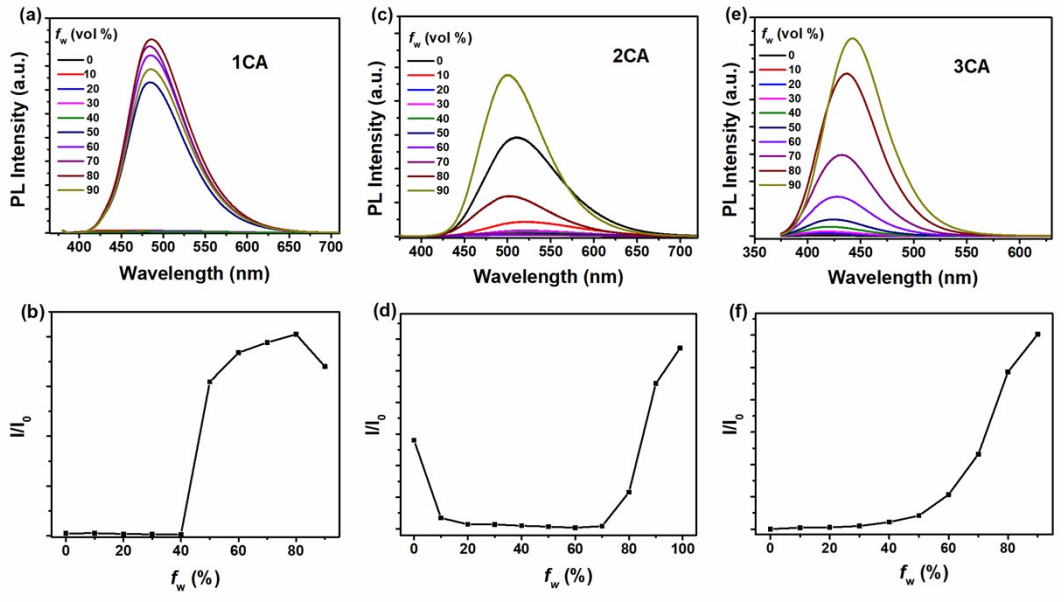

Fig. S8 Emission spectra of (a) **1CA**, (c) **2CA**, (e) **3CA** in the mixture of acetone/H_2O (25 μM, f_w from 0 to 90%) and the corresponding variations in PL intensity (I/I_0) of (b) **1CA**, (d) **2CA**, (f) **3CA** with f_w.

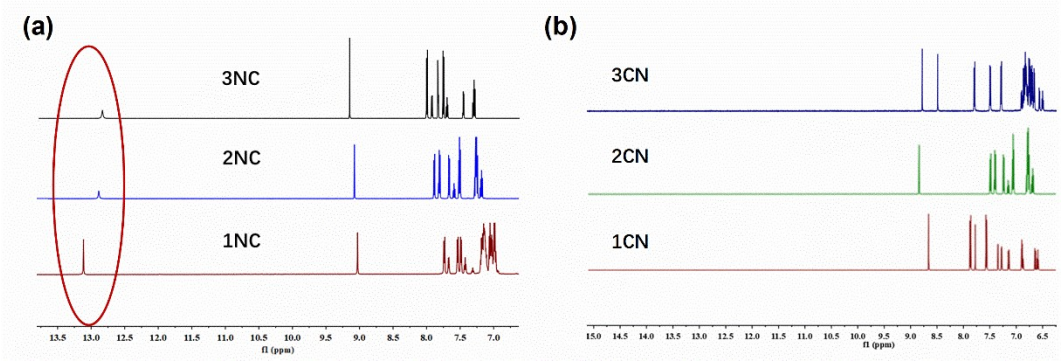

Fig. S9 Partial ^{1}H NMR spectra of (a) **1–3NC** and (b) **1–3CN**.

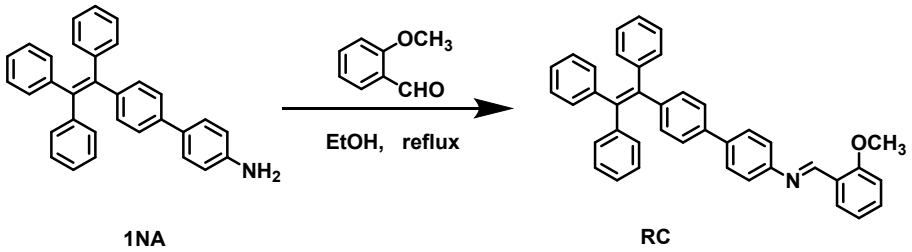

1NA **RC**

Fig. S10 Synthetic routes of compound **RC**.

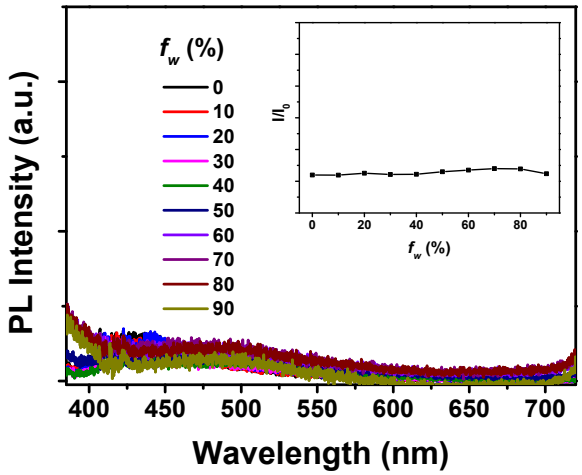

Fig. S11 Emission spectra of **RC** in the mixture of acetone/H_2O (25 μM, f_w from 0 to 90%). Inset: Variations in PL intensity (I/I_0) with f_w.

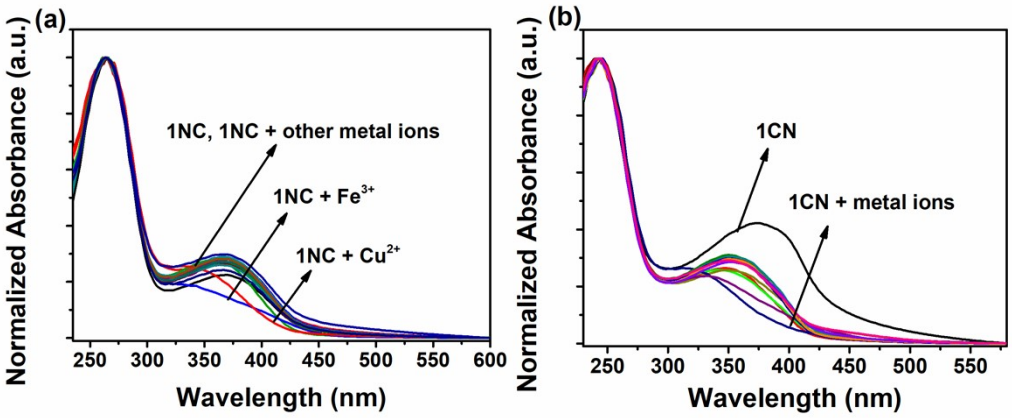

Fig. S12 Absorption spectra of (a) **1NC** (25 μM) and (b) **1CN** (25 μM) towards metal ions (10 mM) in acetone/H_2O mixture (v: v, 1: 99).

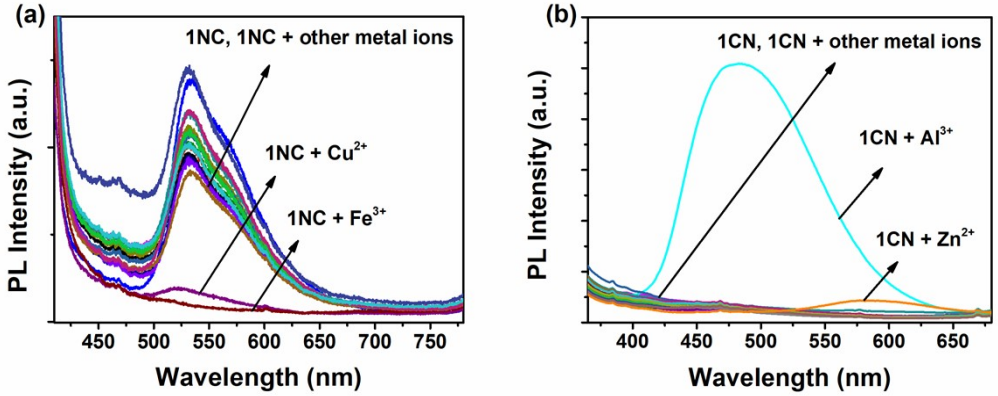

Fig. S13 Emission spectra of the test papers made of (a) **1NC** (25 μM) and (b) **1CN** (25 μM) dripped with various metal ions.

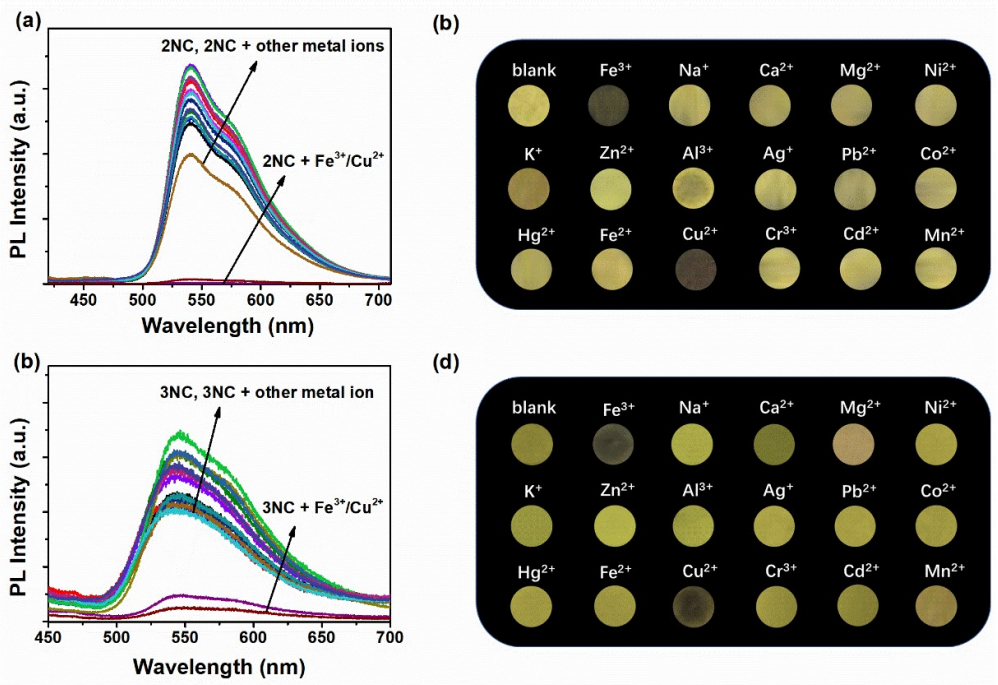

Fig. S14 Absorption spectra of (a) **2NC** (25 μM) and (b) **3NC** (25 μM) towards metal ions (10 mM) in acetone/ H_2O mixture (v: v, 1: 99). The images of (c) **2NC** and (d) **3NC** towards metal ions on test papers.

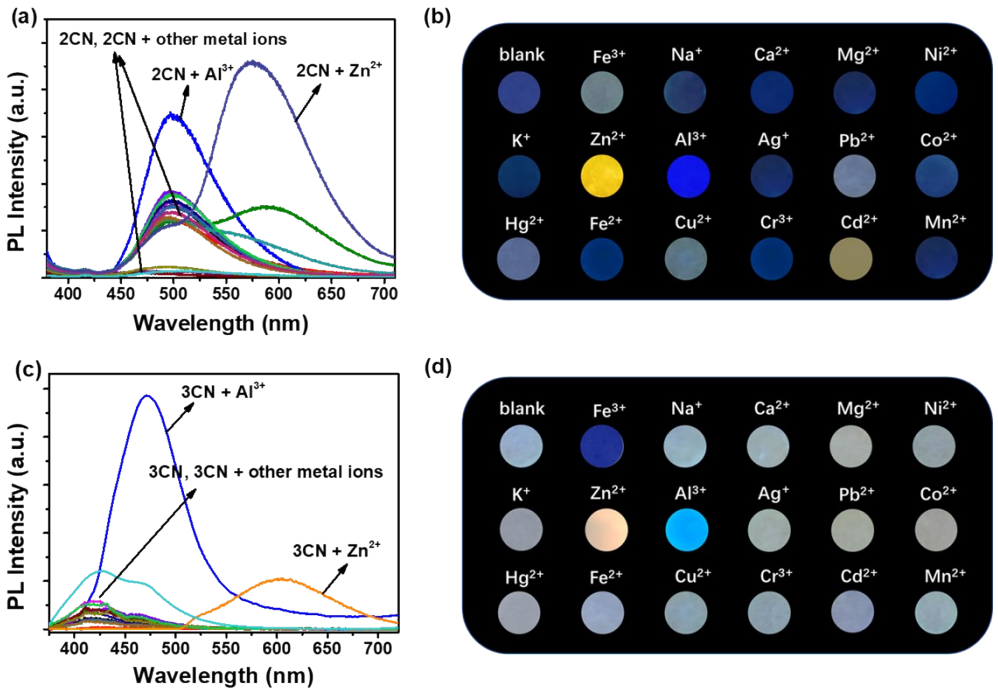

Fig. S15 Absorption spectra of (a) **2CN** (25 μM) and (b) **3CN** (25 μM) towards metal ions (10 mM) in acetone/H_2O mixture (v: v, 1: 99). The images of (c) **2CN** and (d) **3CN** towards metal ions on test papers.

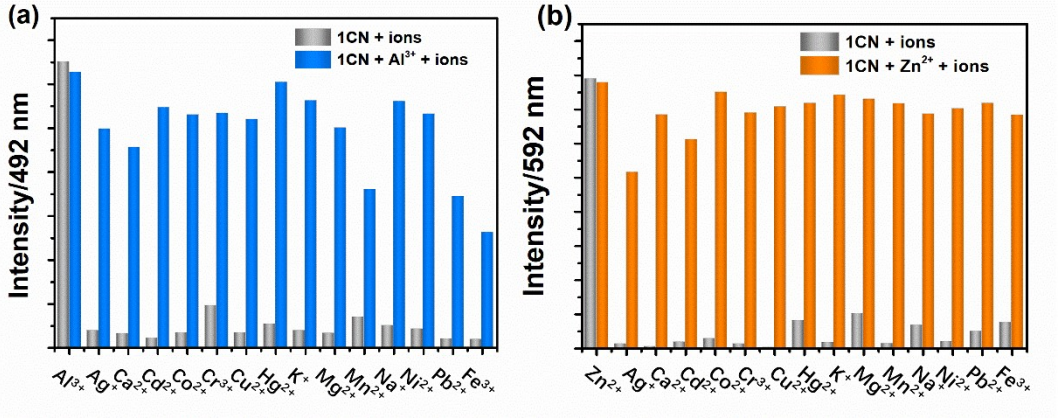

Fig. S16 PL intensity of **1CN** (25 μM) at (a) 492 nm and (b) 592 nm in the presence of other competing metal ions (10 mM) before and after adding Al^{3+} (10 mM) and Zn^{2+} (10 mM) in acetone/H_2O mixture (v: v, 1: 99), respectively.

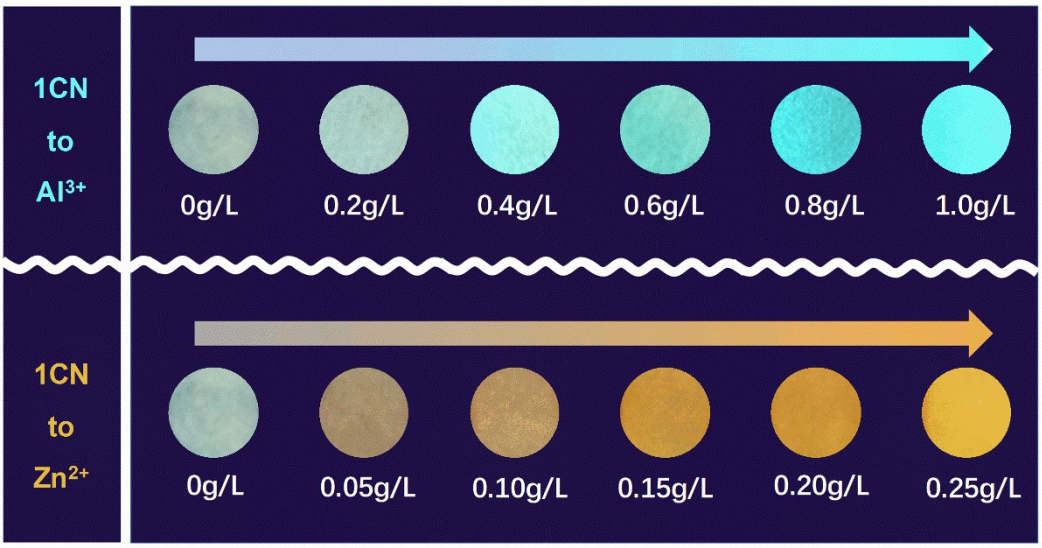

Fig. S17 Fluorescent colorimetric cards for detection of Al^{3+} and Zn^{2+}.

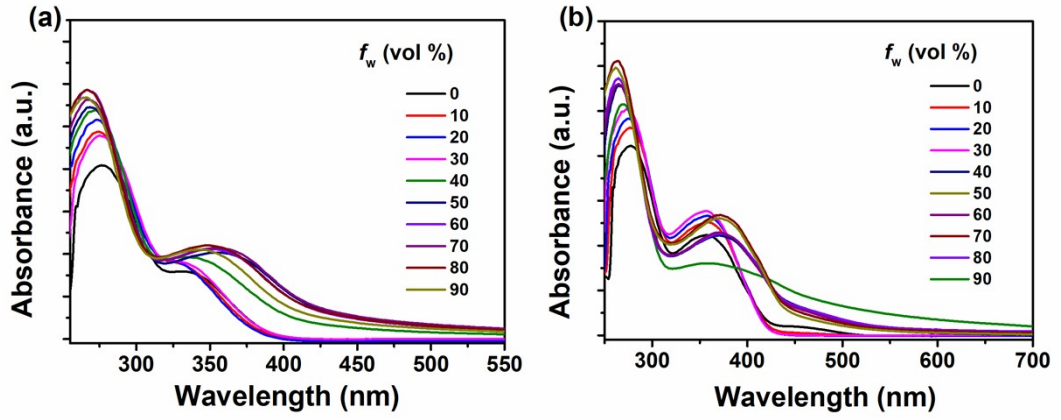

Fig. S18 Absorption spectra of (a) **1CN** (25 μM) with Al^{3+} (10 mM) and (b) Zn^{2+} (10 mM) in the mixture of acetone/H_2O (f_w from 0 to 90%).

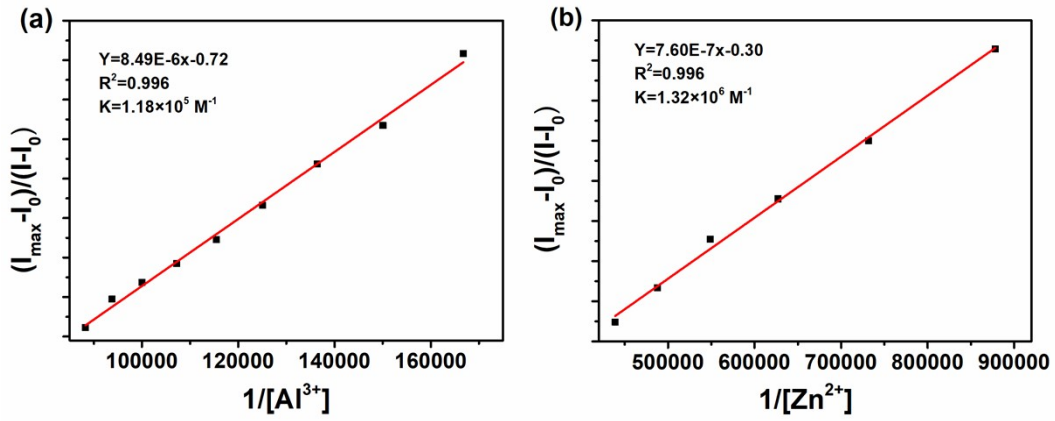

Fig. S19 Benesi-Hildebrand plot of **1CN** towards (a) Al^{3+} and (b) Zn^{2+}.

3. Tables

Table S1 Crystal data and structure refinement for **1NC CCDC: 2107085**

Identification code	**1NC**
Empirical formula	$C_{39}H_{29}NO$
Formula weight	527.63
Temperature/K	202(40)
Crystal system	monoclinic
Space group	$P2_1/n$

a/Å	9.9207(3)
b/Å	9.2558(3)
c/Å	61.9023(18)
α/°	90.00
β/°	90.167(3)
γ/°	90.00
Volume/Å^3	5684.1(3)
Z	8
ρ_{calc}g/cm^3	1.233
μ/mm^{-1}	0.563
F(000)	2224.0
Crystal size/mm^3	0.07 × 0.02 × 0.01
Radiation	CuKα (λ = 1.54184)
2Θ range for data collection/°	8.58 to 139.88
Index ranges	-11 ≤ h ≤ 11, -11 ≤ k ≤ 7, -74 ≤ l ≤ 65
Reflections collected	23812
Independent reflections	10543 [R_{int} = 0.0382, R_{sigma} = 0.0487]
Data/restraints/parameters	10543/43/768
Goodness-of-fit on F^2	1.108
Final R indexes [I>=2σ (I)]	R_1 = 0.0885, wR_2 = 0.1989
Final R indexes [all data]	R_1 = 0.1009, wR_2 = 0.2053
Largest diff. peak/hole / e Å^{-3}	0.41/-0.39

Table S2 Crystal data and structure refinement for **1CN CCDC: 2107068**

Identification code	**1CN**
Empirical formula	$C_{78}H_{58}N_2O_2$

Formula weight	1055.26
Temperature/K	293.63(10)
Crystal system	monoclinic
Space group	$P2_1/n$
a/Å	9.9949(7)
b/Å	9.4404(9)
c/Å	61.749(5)
α/°	90.00
β/°	91.980(7)
γ/°	90.00
Volume/Å^3	5822.8(8)
Z	4
ρ_{calc}g/cm^3	1.204
μ/mm^{-1}	0.550
F(000)	2224.0
Crystal size/mm^3	0.09 × 0.07 × 0.03
Radiation	CuKα (λ = 1.54184)
2Θ range for data collection/°	8.6 to 142.38
Index ranges	$-6 \leq h \leq 11$, $-11 \leq k \leq 10$, $-74 \leq l \leq 69$
Reflections collected	21827
Independent reflections	10708 [R_{int} = 0.0525, R_{sigma} = 0.0831]
Data/restraints/parameters	10708/0/741
Goodness-of-fit on F^2	1.034
Final R indexes [I>=2σ (I)]	R_1 = 0.0930, wR_2 = 0.2058
Final R indexes [all data]	R_1 = 0.1319, wR_2 = 0.2317
Largest diff. peak/hole / e Å^{-3}	0.26/-0.28

Table S3 Crystal data and structure refinement for **2NC CCDC: 2107082**

Identification code	**2NC**
Empirical formula	$C_{62}H_{48}N_4O_2$
Formula weight	881.04
Temperature/K	301.95(10)
Crystal system	monoclinic
Space group	$P2_1/c$
a/Å	26.9099(11)
b/Å	9.5273(3)
c/Å	19.2556(8)
α/°	90
β/°	108.442(4)
γ/°	90
Volume/Å^3	4683.2(3)
Z	4
ρ_{calc}g/cm^3	1.250
μ/mm^{-1}	0.076
F(000)	1856.0
Crystal size/mm^3	0.12 × 0.07 × 0.05
Radiation	Mo Kα (λ = 0.71073)
2Θ range for data collection/°	4.234 to 62.18
Index ranges	$-33 \leq h \leq 30$, $-13 \leq k \leq 11$, $-23 \leq l \leq 24$
Reflections collected	45770
Independent reflections	11907 [R_{int} = 0.0415, R_{sigma} = 0.0425]

Data/restraints/parameters	11907/30/615
Goodness-of-fit on F^2	1.052
Final R indexes [I>=2σ (I)]	R_1 = 0.0553, wR_2 = 0.1524
Final R indexes [all data]	R_1 = 0.1073, wR_2 = 0.1828
Largest diff. peak/hole / e $Å^{-3}$	0.15/-0.26

Table S4 Crystal data and structure refinement for **2CN CCDC: 2107078**

Identification code	**2CN**
Empirical formula	$C_{62}H_{48}N_4O_2$
Formula weight	881.04
Temperature/K	302.00(10)
Crystal system	triclinic
Space group	P-1
a/Å	10.3835(6)
b/Å	10.7250(6)
c/Å	24.4935(12)
α/°	77.553(4)
β/°	79.932(5)
γ/°	63.410(5)
Volume/$Å^3$	2372.2(2)
Z	2
$\rho_{calc}g/cm^3$	1.233
μ/mm^{-1}	0.075
F(000)	928.0
Crystal size/mm^3	0.08 × 0.05 × 0.04
Radiation	Mo Kα (λ = 0.71073)

2Θ range for data collection/°	3.42 to 62.012
Index ranges	$-14 \leq h \leq 13$, $-14 \leq k \leq 13$, $-33 \leq l \leq 30$
Reflections collected	29160
Independent reflections	11743 [R_{int} = 0.0373, R_{sigma} = 0.0576]
Data/restraints/parameters	11743/0/633
Goodness-of-fit on F^2	1.023
Final R indexes [I>=2σ (I)]	R_1 = 0.0699, wR_2 = 0.1611
Final R indexes [all data]	R_1 = 0.1567, wR_2 = 0.1918
Largest diff. peak/hole / e $Å^{-3}$	0.20/-0.19

Table S5 Crystal data and structure refinement for **3NC CCDC: 2120445**

Identification code	LD_1_3_autored
Empirical formula	$C_{34}H_{26}N_2O_2S_2$
Formula weight	558.730
Temperature/K	N/A
Crystal system	monoclinic
Space group	I2
a/Å	7.3383(2)
b/Å	6.1634(2)
c/Å	60.9206(16)
α/°	90
β/°	93.020(2)
γ/°	90
Volume/$Å^3$	2751.54(14)
Z	4

ρ_{calc}g/cm^3	1.349
μ/mm^{-1}	2.031
F(000)	1173.9
Crystal size/mm^3	0.09 × 0.04 × 0.01
Radiation	Cu Kα (λ = 1.54184)
2Θ range for data collection/°	5.82 to 154.92
Index ranges	-9 ≤ h ≤ 8, -7 ≤ k ≤ 7, -74 ≤ l ≤ 75
Reflections collected	14483
Independent reflections	5162 [R_{int} = 0.0770, R_{sigma} = 0.0503]
Data/restraints/parameters	5162/2/363
Goodness-of-fit on F^2	1.116
Final R indexes [I>=2σ (I)]	R_1 = 0.0923, wR_2 = 0.2607
Final R indexes [all data]	R_1 = 0.1022, wR_2 = 0.2731
Largest diff. peak/hole / e Å^{-3}	0.83/-0.46

Table S6 Crystal data and structure refinement for **3CN CCDC: 2107090**

Identification code	**3CN**
Empirical formula	$C_{17}H_{13}NOS$
Formula weight	279.34
Temperature/K	293(2)
Crystal system	triclinic
Space group	P-1
a/Å	5.9514(7)
b/Å	16.012(3)
c/Å	16.264(4)
α/°	63.516(19)

β/°	82.231(14)
γ/°	85.875(12)
Volume/Å^3	1374.4(5)
Z	4
ρ_{calc}g/cm^3	1.350
μ/mm^{-1}	2.033
F(000)	584.0
Crystal size/mm^3	0.17 × 0.14 × 0.02
Radiation	CuKα (λ = 1.54184)
2Θ range for data collection/°	10.434 to 133.17
Index ranges	-7 ≤ h ≤ 4, -18 ≤ k ≤ 19, -18 ≤ l ≤ 19
Reflections collected	7995
Independent reflections	4659 [R_{int} = 0.0339, R_{sigma} = 0.0518]
Data/restraints/parameters	4659/0/369
Goodness-of-fit on F^2	1.047
Final R indexes [I>=2σ (I)]	R_1 = 0.0612, wR_2 = 0.1701
Final R indexes [all data]	R_1 = 0.0836, wR_2 = 0.2050
Largest diff. peak/hole / e Å^{-3}	0.37/-0.47

Table S7 Recovery study of **1CN** to Al^{3+} in spiked water samples.

Sample	Al^{3+} spiked (M)	Al^{3+} recovered (M)	Recovery (%)	Standard error(%)	RSD
	6.00×10^{-6}	5.84×10^{-6}	97.3	2.7	0.057
	9.00×10^{-6}	8.73×10^{-6}	97.0	3.0	0.066
Tap water	1.20×10^{-5}	1.22×10^{-5}	101.7	1.7	0.081
	1.50×10^{-5}	1.51×10^{-5}	100.5	0.5	0.108
	1.80×10^{-5}	1.78×10^{-5}	98.8	1.2	0.041
	6.00×10^{-6}	5.89×10^{-6}	98.1	1.9	0.054
	9.00×10^{-6}	9.00×10^{-6}	100.0	0	0.100
Drinking water	1.20×10^{-5}	1.22×10^{-6}	101.9	1.9	0.128
	1.50×10^{-5}	1.47×10^{-5}	98.0	2.0	0.048
	1.80×10^{-5}	1.79×10^{-5}	99.5	0.8	0.110
	6.00×10^{-6}	6.02×10^{-6}	100.4	0.4	0.075
	9.00×10^{-6}	8.88×10^{-6}	98.7	1.3	0.060
River water	1.20×10^{-5}	1.17×10^{-6}	97.8	2.2	0.027
	1.50×10^{-5}	1.47×10^{-5}	98.0	2.0	0.106
	1.80×10^{-5}	1.76×10^{-5}	97.8	2.2	0.033

Table S8 Recovery study of **1CN** to Zn^{2+} in spiked water samples.

Sample	Zn^{2+} spiked (M)	Zn^{2+} recovered (M)	Recovery (%)	Standard error(%)	RSD
	3.00×10^{-6}	2.93×10^{-6}	97.6	2.4	0.070
	6.00×10^{-6}	6.15×10^{-6}	102.5	2.5	0.058
Tap water	9.00×10^{-6}	8.57×10^{-6}	98.7	1.3	0.090
	1.20×10^{-5}	1.14×10^{-5}	97.6	2.4	0.081
	1.50×10^{-5}	1.55×10^{-5}	103.1	3.1	0.106
	3.00×10^{-6}	3.12×10^{-6}	102.5	2.5	0.055
	6.00×10^{-6}	6.10×10^{-6}	101.6	1.6	0.067
Drinking water	9.00×10^{-6}	9.09×10^{-6}	101.0	1.0	0.031
	1.20×10^{-5}	1.22×10^{-5}	102.0	2.0	0.093
	1.50×10^{-5}	1.54×10^{-5}	102.5	2.5	0.042
	3.00×10^{-6}	3.05×10^{-6}	101.5	1.5	0.046
	6.00×10^{-6}	6.04×10^{-6}	100.6	0.6	0.064
River water	9.00×10^{-6}	8.82×10^{-6}	98.0	2.0	0.054
	1.20×10^{-5}	1.19×10^{-5}	98.9	1.1	0.116
	1.50×10^{-5}	1.49×10^{-5}	99.7	0.3	0.079

4. ^{1}H NMR and ^{13}C NMR

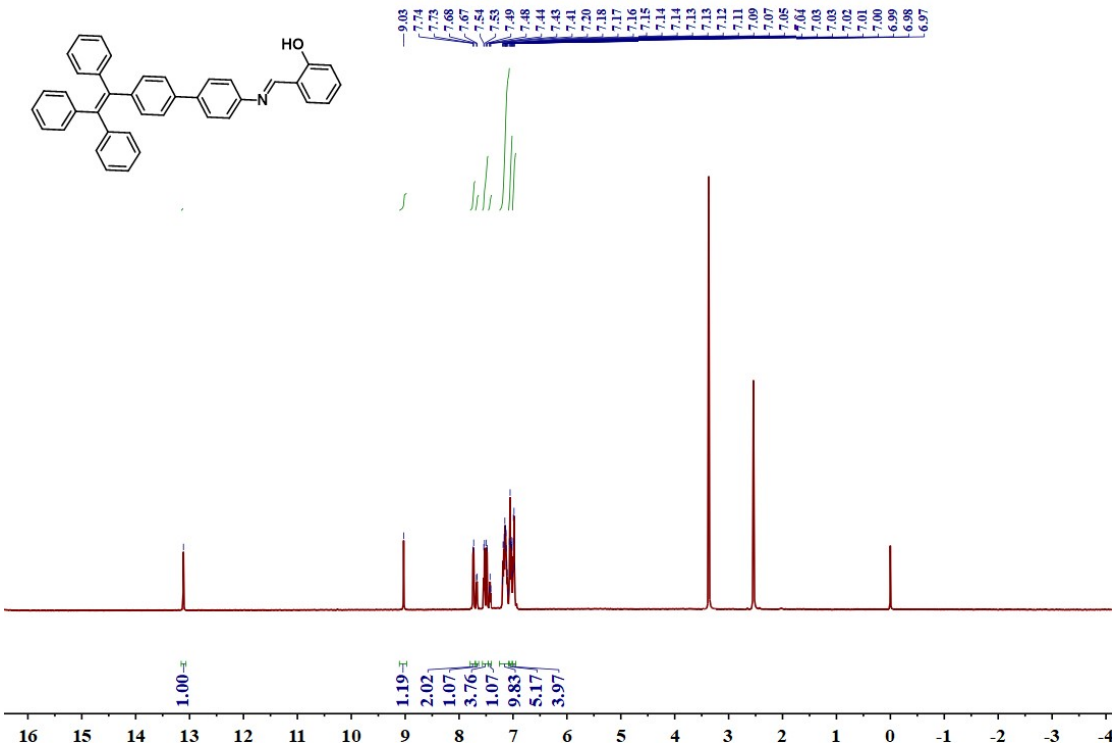

Fig. S20 ^{1}H NMR spectrum of **1NC** in DMSO-*d*6.

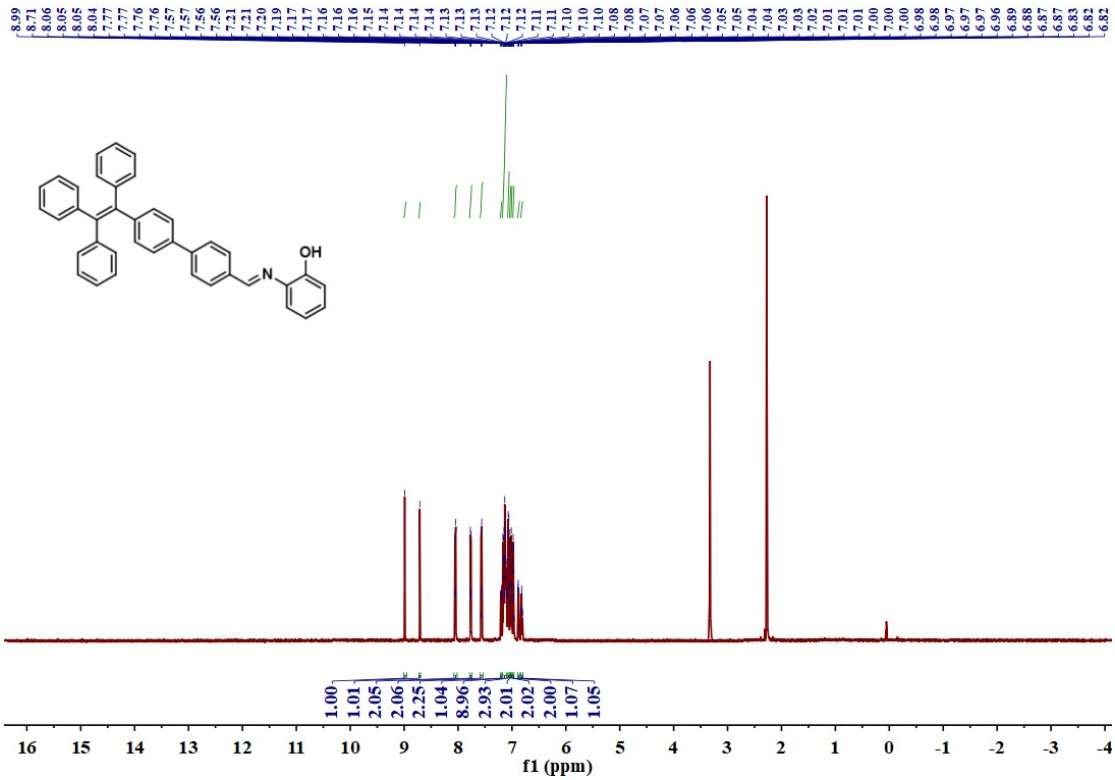

Fig. S21 ^{1}H NMR spectrum of **1CN** in DMSO-*d*6.

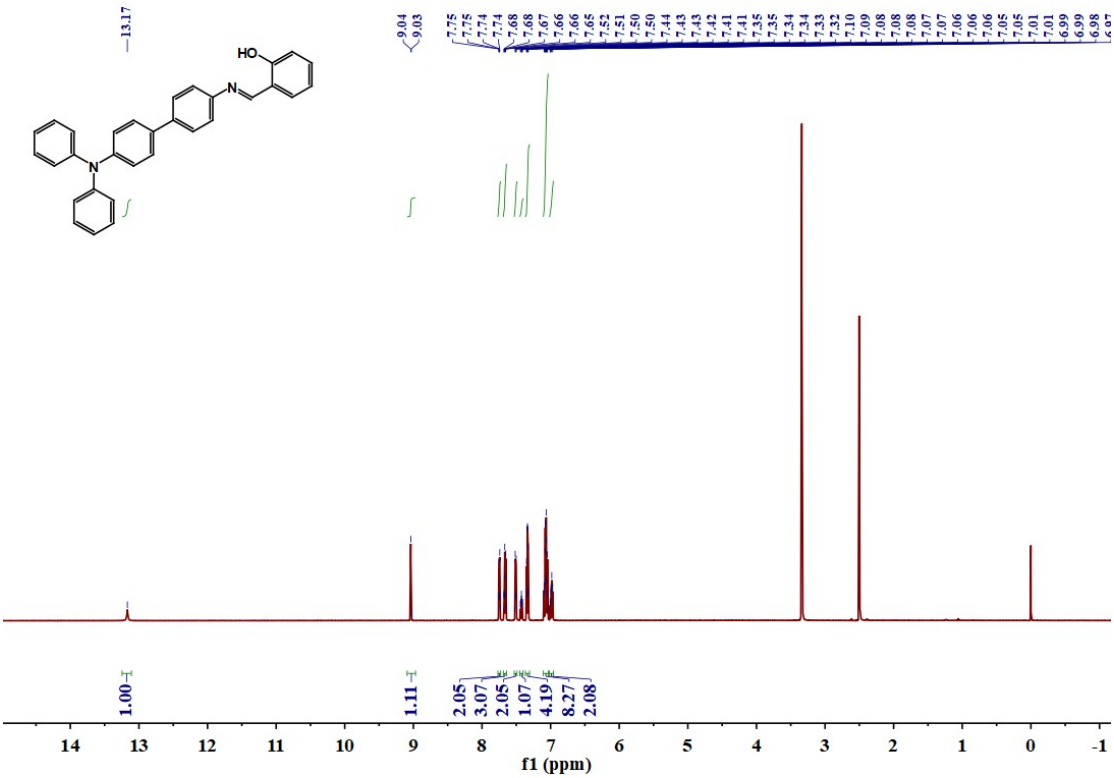

Fig. S22 ^{1}H NMR spectrum of **2NC** in DMSO-*d*6.

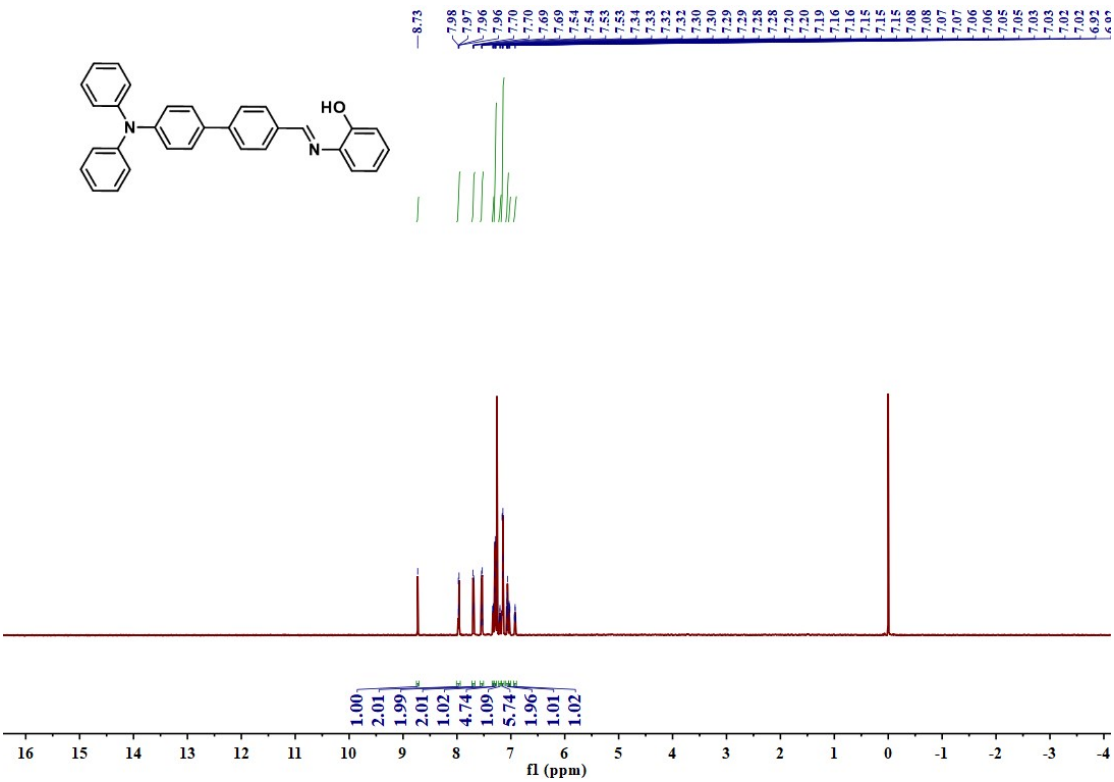

Fig. S23 ^{1}H NMR spectrum of **2CN** in $CDCl_3$.

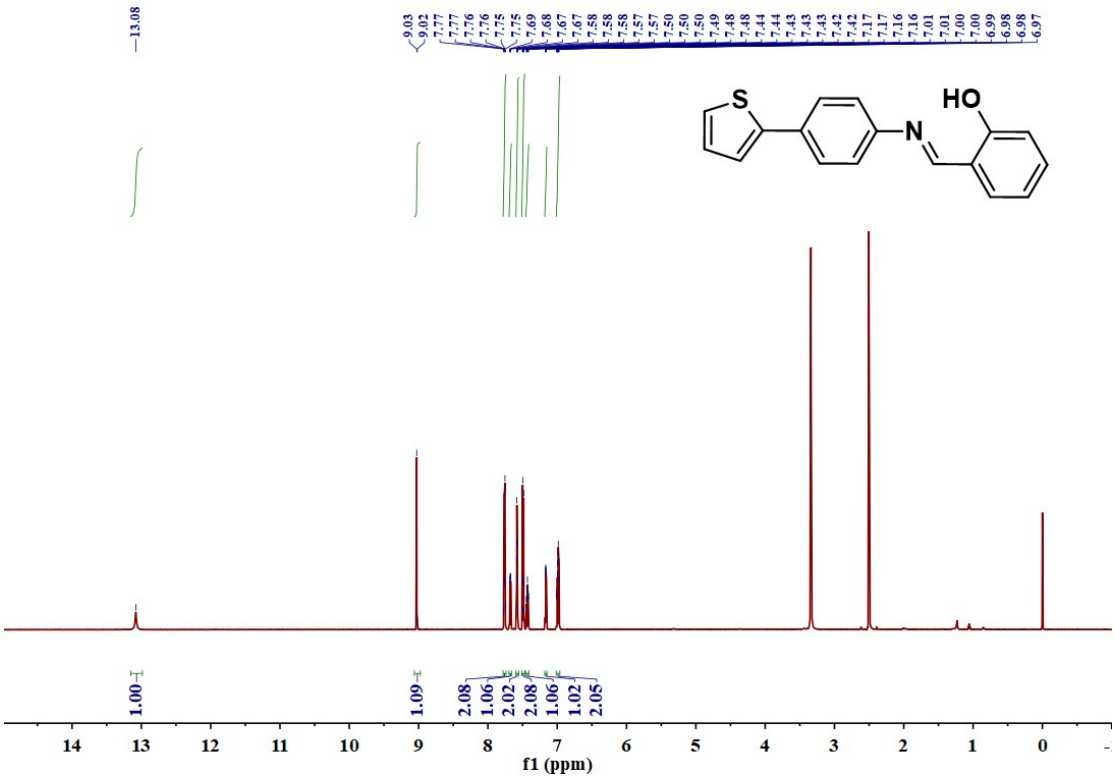

Fig. S24 ^{1}H NMR spectrum of **3NC** in DMSO-*d*6.

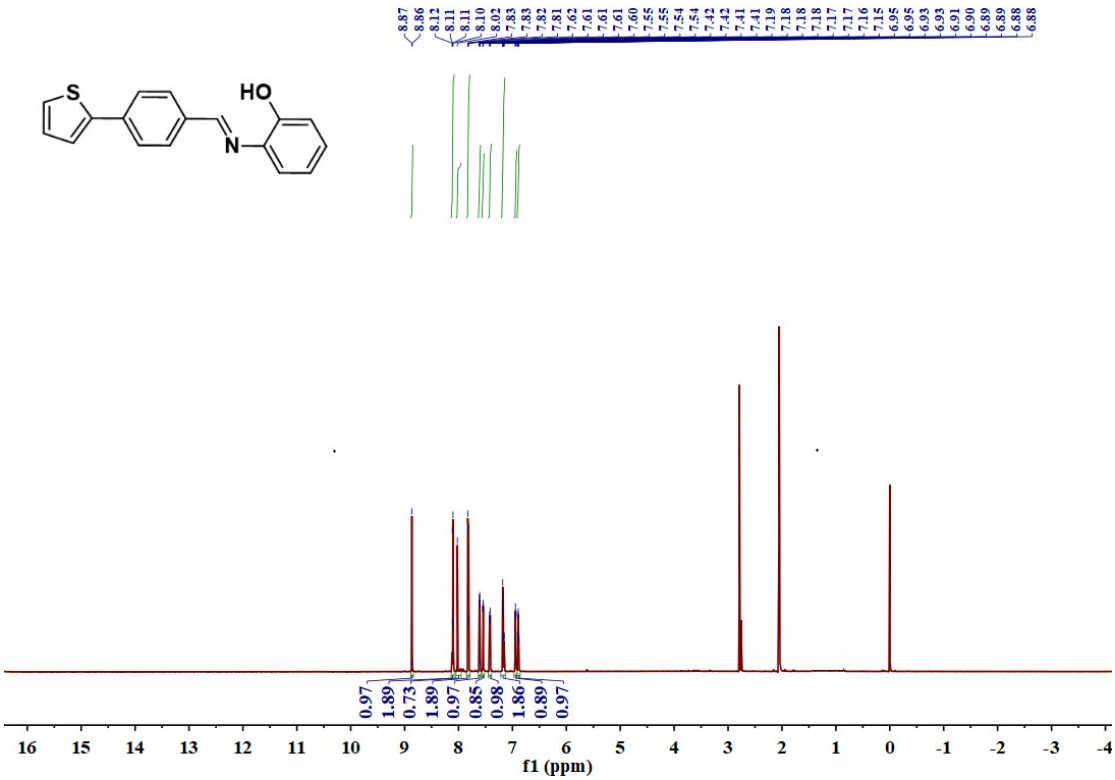

Fig. S25 ^{1}H NMR spectrum of **3CN** in acetone-*d*6.

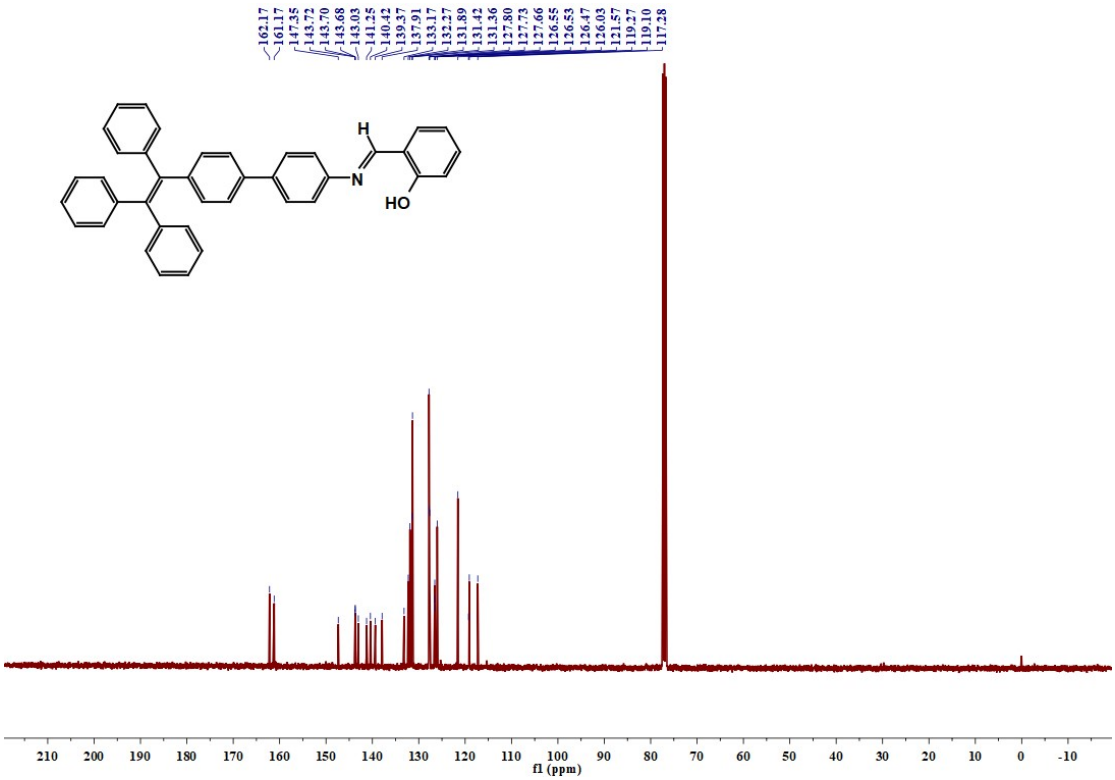

Fig. S26 ^{13}C NMR spectrum of **1NC** in $CDCl_3$.

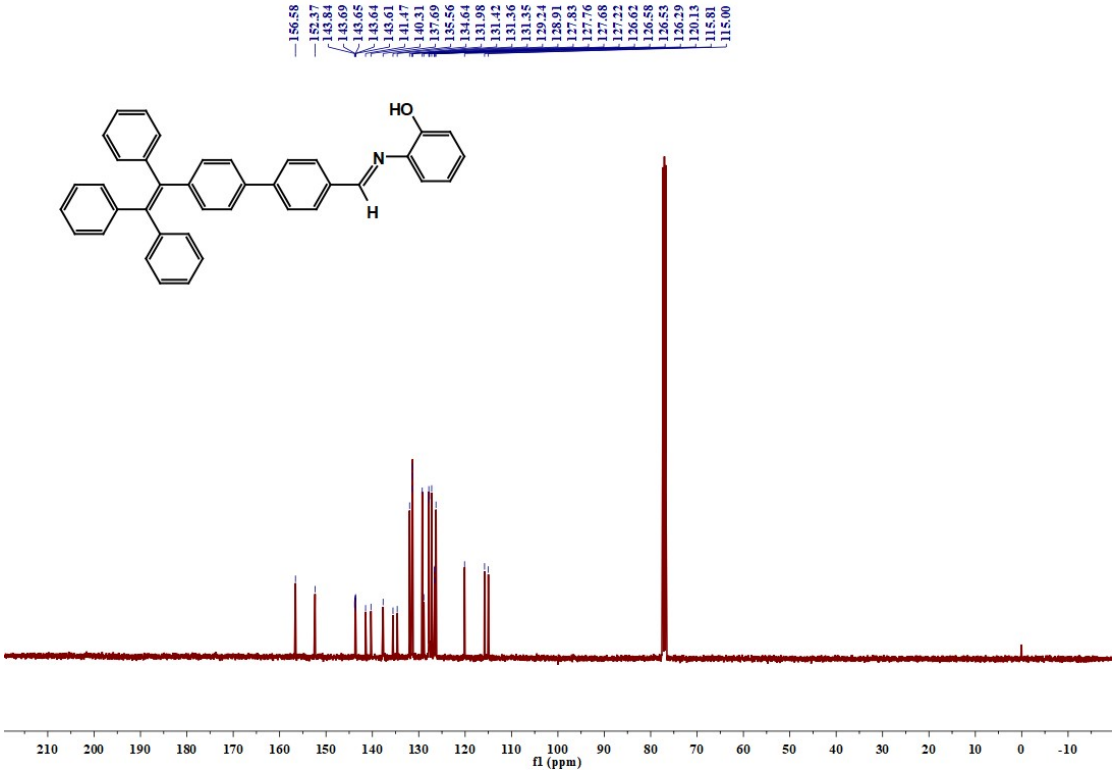

Fig. S27 ^{13}C NMR spectrum of **1CN** in $CDCl_3$.

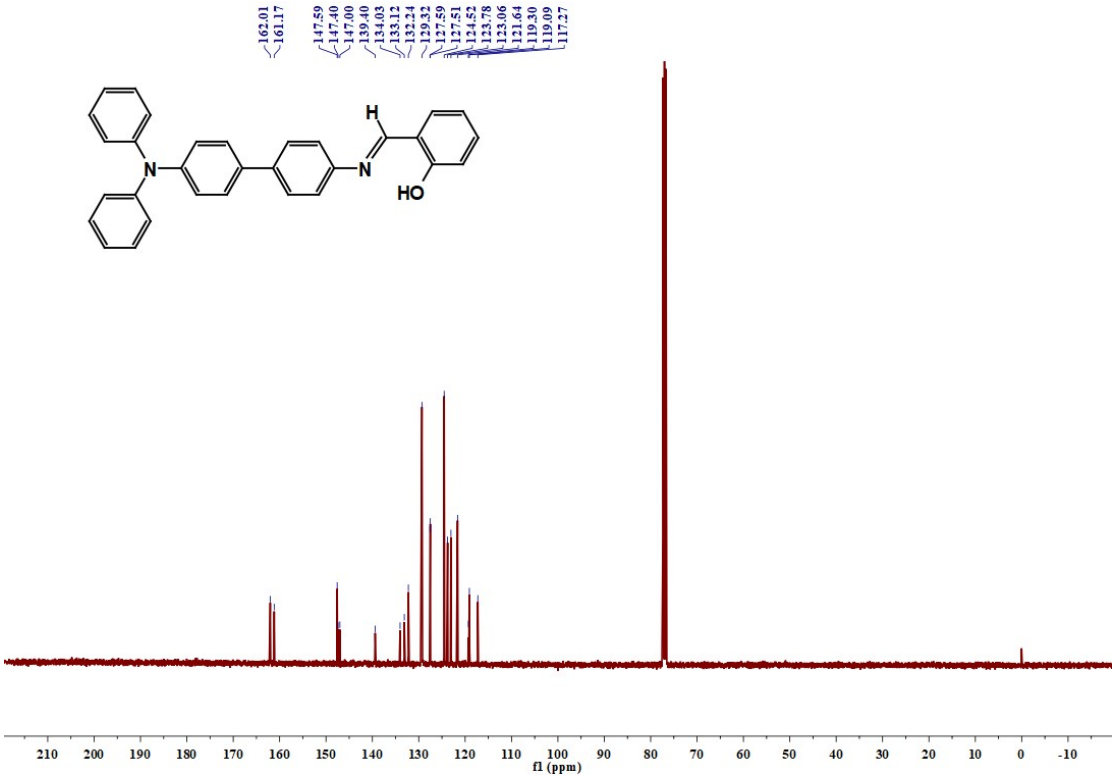

Fig. S28 ^{13}C NMR spectrum of **2NC** in $CDCl_3$.

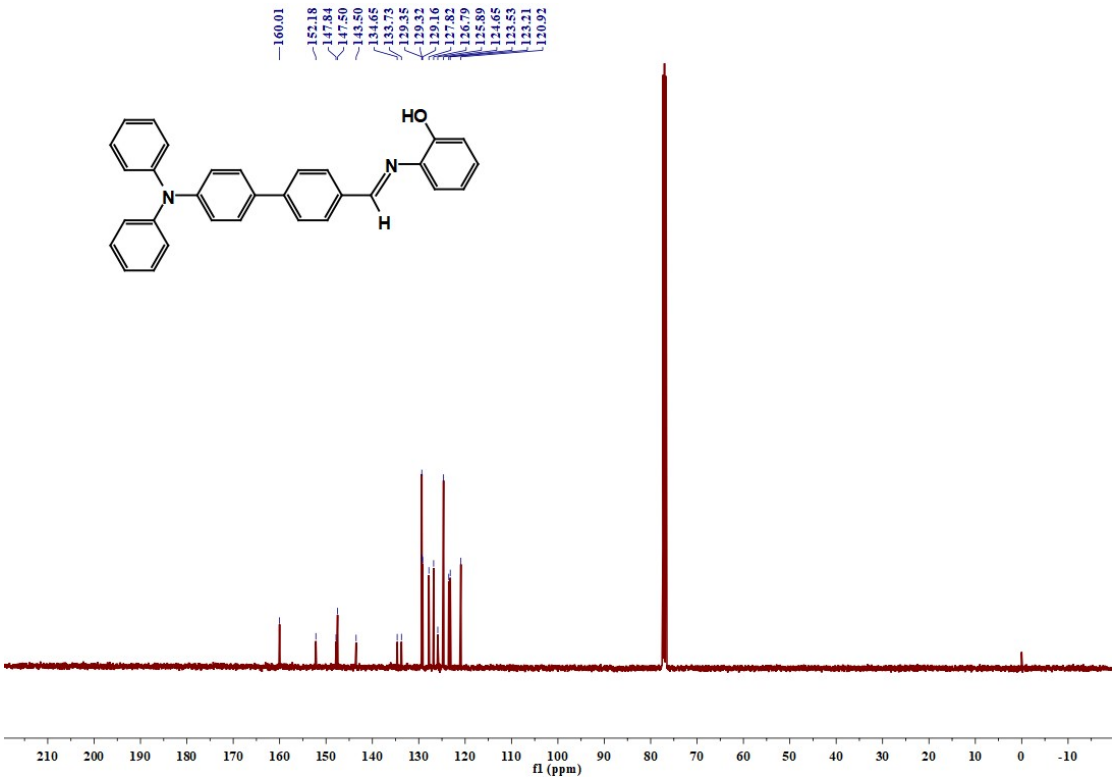

Fig. S29 ^{13}C NMR spectrum of **2CN** in $CDCl_3$.

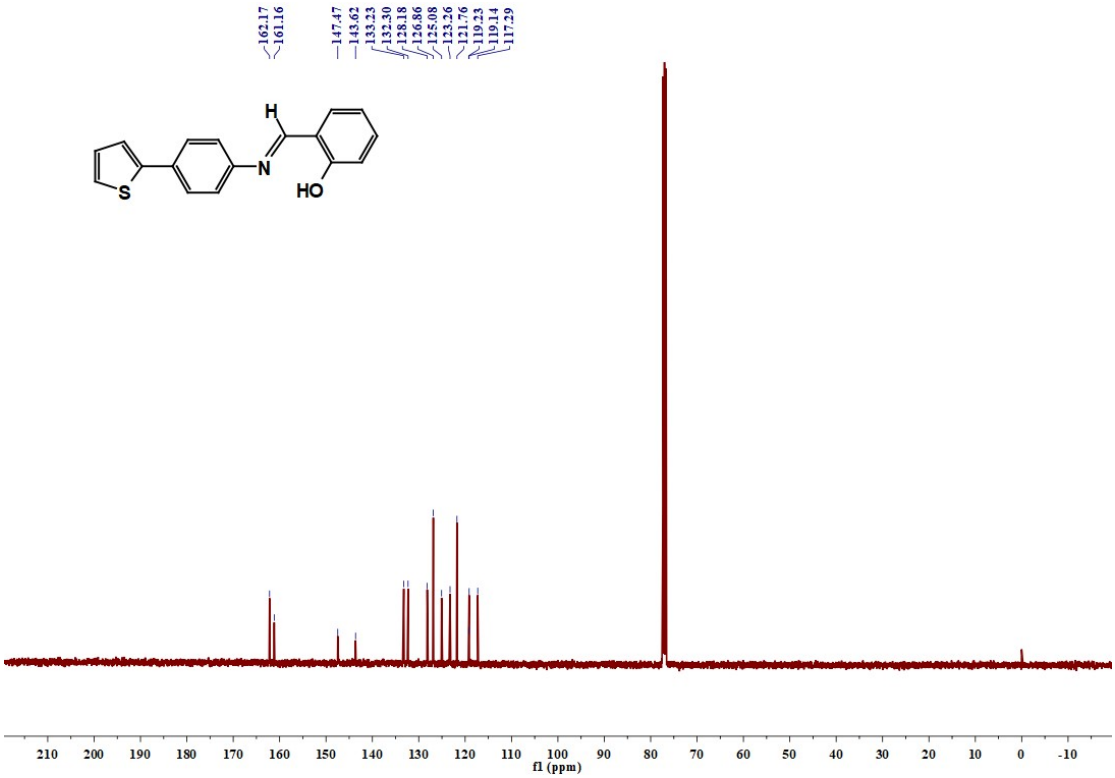

Fig. S30 ^{13}C NMR spectrum of **3NC** in $CDCl_3$.

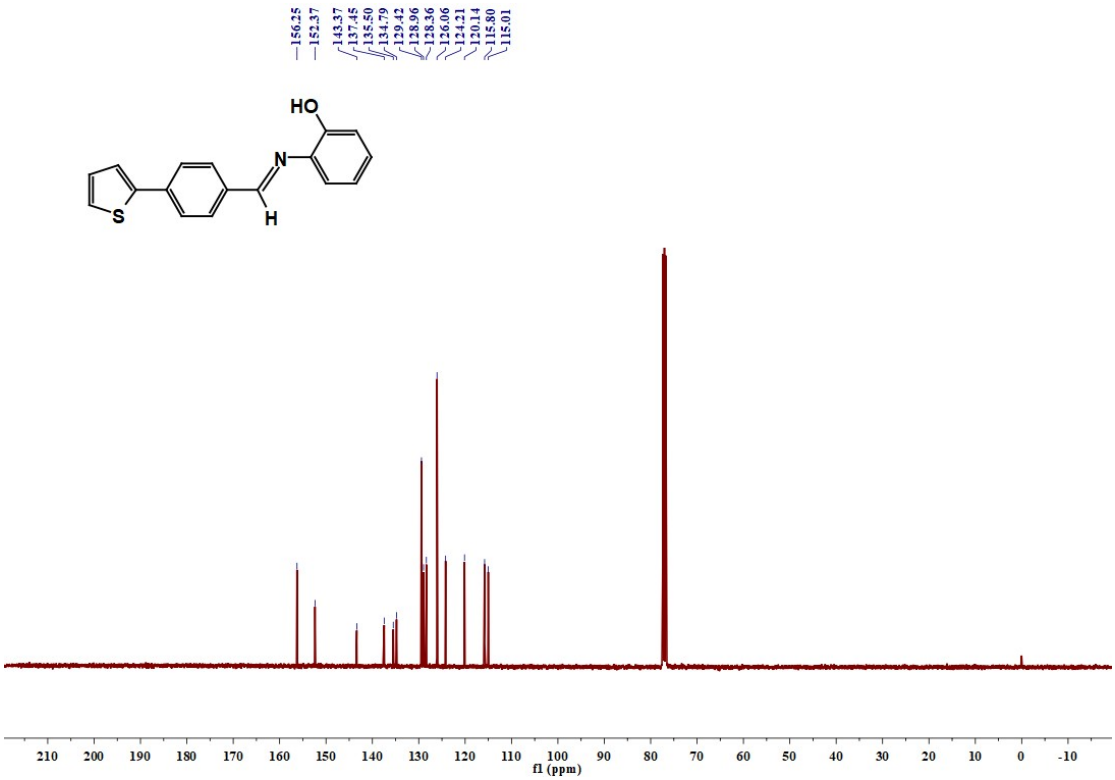

Fig. S31 ^{13}C NMR spectrum of **3CN** in $CDCl_3$.

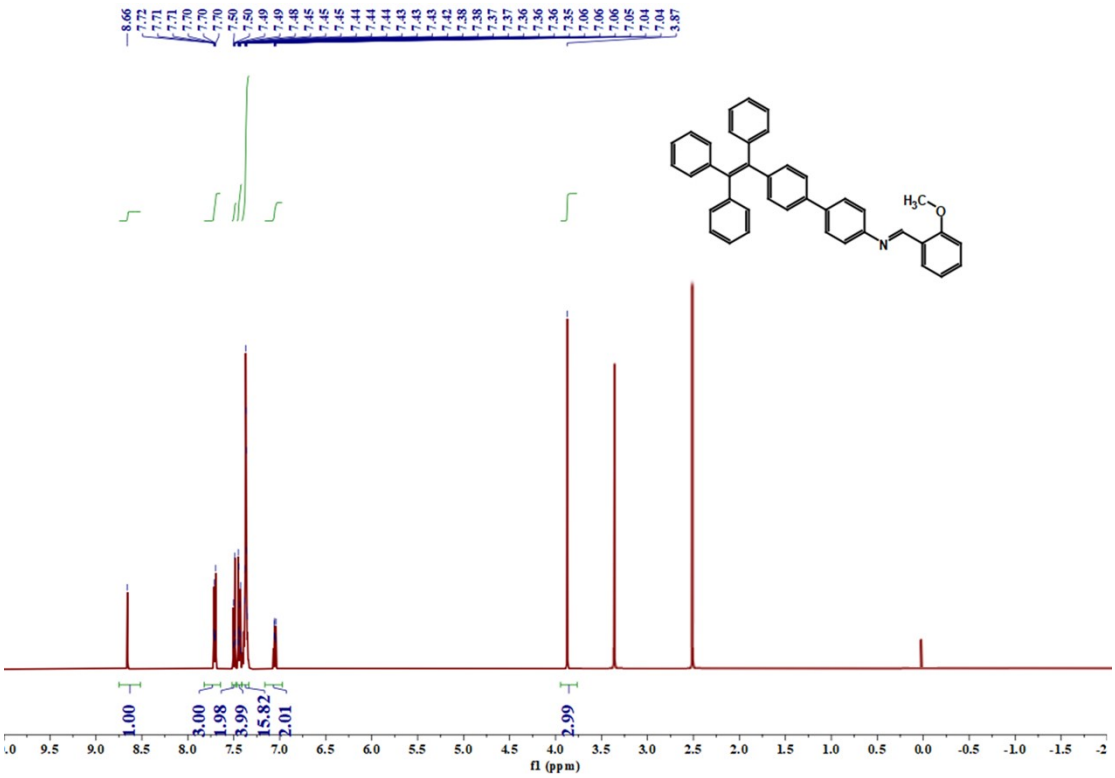

Fig. S32 ^{1}H NMR spectrum of **RC** in DMSO-*d6*.

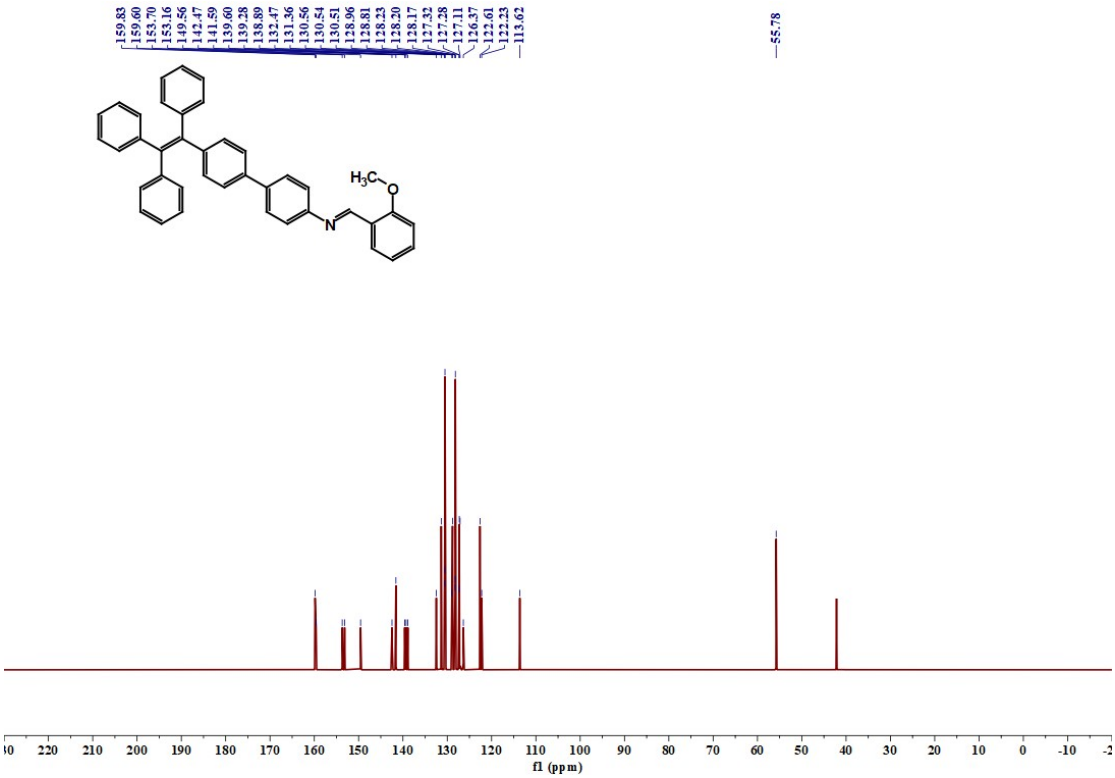

Fig. S33 ^{13}C NMR spectrum of **RC** in DMSO-*d6*.